Characterization of Unbounded Multiport Microstrip Passive Circuits Using an Explicit Network-Based Method of Moments

Lei Zhu, *Member, IEEE,* and Ke Wu, *Senior Member, IEEE*

***Abstract*—This paper is concerned with a field–theoretical characterization of unbounded multiport microstrip passive circuits using an explicit network technique. The cornerstone of this efficient modeling framework is based on a method of moments (MoM) that makes use of the explicit representation of a generalized matrix of network parameter. To physically formulate the equivalent multiport network for a multiport circuit, a delta-gap voltage source backed by a vertical electric wall is conceptually introduced to terminate each port. In this way, the multiport microstrip circuit to be modeled is externally connected at an adequate location. The image principle is applied at the port to remove the electric wall and the open environment can effectively be simulated. With the unified impressed delta-gap source model and appropriate partition of the entire multiport circuit topology, a MoM procedure is developed and applied to extract the network parameters directly from the field–theoretical formulations. All possible physical phenomena such as radiation and leakage losses are incorporated in the algorithm. Two distinctive examples presented in this paper demonstrate the effectiveness of the proposed algorithm for handling multilayered multiport passive and antenna circuits. Convergence analysis is made for the filter example compared with experimental results, showing that the proposed algorithm is very stable and accurate. Theoretical and experimental results indicates that the implicit unbounded effects may be influential on electrical performance and should be considered in such a field–theoretical modeling and design tool as proposed in this paper.**

***Index Terms*—CAD, experiments, method of moments (MoM), modeling, multiport passive circuit, radiation and leakage losses.**

I. Introduction

RECENT rapid development of monolithic microwave integrated circuits (MMIC's) and planar antenna technology has aroused a considerable interest in exploiting an efficient field–theoretical package for accurate modeling and design of planar passive circuits that may be in the form of multiport and unbounded topology. Among the field–theoretical-based algorithms developed to date, the method of moments (MoM) formulated in the spectral domain or space domain [1]–[14] is considered as one of the most powerful models for comprehensive treatment of various complex planar structures. The clue to the usefulness of such a method is that realistic electromagnetic phenomena, namely, space-wave radiation for open structure and surface-wave leakage for multilayered circuit, can be accurately incorporated without resorting to approximate absorbing-boundary conditions that are commonly used to define a finite window of analysis in the discrete space-domain techniques [15], [16]. So far, the MoM-based full-wave techniques that extract the dyadic Green's function of layered dielectric circuit has successfully been applied to the modeling and design of microstrip-fed patch antenna and other countless passive circuits [1]–[14].

Under the full-wave scheme of the MoM for a unbounded microstrip structure, a generalized integral equation can analytically be formulated for the modal solution of unknown current density flowing over the entire conductor surface, including the microstrip circuit and every port that may be attached with the infinite length of transmission line in the early model. During the 1980's, it was realized that one of the major difficulties was how to mathematically implement a rigorous, but versatile, excitation mechanism [1], [2], [4] that should precisely describe wave propagation at each input and/or output ports, externally connected with the planar circuit. The workable excitation mechanism should be made such that the complexity of current distribution over these ports can be effectively avoided or at least simplified from the point of view of field–theoretical modeling.

To our current knowledge, two types of excitation mechanism [1], [2] (namely, traveling-wave excitation and delta-gap voltage excitation) that were initially proposed for the analysis of open microstrip gap discontinuities have subsequently been used in the modeling of a large variety of unbounded structures, including multiport microstrip circuits [6], [7], [10]–[13]. In the former excitation [2], the current density flowing at each port is expanded into a superposition of incident and reflected semi-infinite traveling-wave functions and thus the relevant scattering parameters can be directly extracted from reinforcing the boundary condition over the conductor surface. While in the latter case [1], a delta voltage source is impressed at each port that is usually located sufficiently far away from the discontinuity of concern so that the modal admittance parameters can be obtained by assuming the vanishing effects of higher order modes. However, the use of the traveling-wave model may lead to some troubles in the practical design of algorithm when a multiport planar circuit is considered [13]. Essentially, the calculation of a convolution of the entire-domain traveling-wave basis functions over each port and the sub-domain sinusoidal weighting functions is much more involved. This procedure degrades the

Manuscript received June 20, 1997; revised August 22, 1997. This work was supported by the Natural Sciences and Engineering Research Council (NSERC) of Canada.

The authors are with the Poly-Grames Research Center, Departement de Génie Electrique et de Génie Informatique, École Polytechnique de Montréal, Montréal, P.Q., Canada H3C 3A7.

Publisher Item Identifier S 0018-9480(97)08244-6.

numerical efficiency of the complete algorithm such as the time-consuming and relative inconvenience.

On the other hand, the delta-gap voltage model requires an additional calculation to obtain the network parameters from the precalculated standing-wave current-density pattern along the line of each port. Therefore, such a model presents no attractiveness for handling a multiport structure. To remedy this defect, an alternative technique that uses a matched load [17], [18] has recently been proposed for the extraction of S-parameters from knowing the current profile at each port of an open multiport structure. Despite its obvious advantages, this technique requires M-step calculations for an M-port structure to obtain the complete solution of S-parameters. In other words, this indirect technique is quite similar to the traveling-wave model [1]. Likewise, it is still attractive to use its simple and accurate excitation mechanism for the explicit modeling of network parameters if the number of ports is a primary factor of concern.

Considering the fact that the circuit substrate in most practical designs is chosen to be electrically thin in order to suppress unwanted parasitic radiation loss and element-to-element spurious coupling, unbounded microstrip circuits may be reasonably assumed to be enclosed within an electrically large shielding box without sacrificing the accuracy of results. As such, a deterministic MoM based on the source-excitation model can be effectively used to characterize these microstrip circuits [3], [4], [8]. One of the typical procedures is to impress a delta-gap voltage source or a current source at the excited terminal of a related port that simulates a probe-fed excitation. In this way, the network parameters can be explicitly extracted from the calculated complex magnitude of basis function defined at the terminals of all ports. But, the use of this model is limited only to the shielded planar passive circuits. Very recently, the delta-gap voltage source and the impressed-current source have theoretically been proved to be equivalent, and they have been successfully applied for systematic network characterization of shielded multiport circuits [19]. Nevertheless, a number of challenging issues that remain need to be addressed, one of which is how to handle the open environment of a unbounded structure. This prompts the search for a simple and unified model for these complex topologies of circuit.

Using the delta-gap voltage-source model, a simple and feasible scheme was proposed in [20] to explicitly formulate the input impedance of microstrip-fed patch antenna. In that case, our attention was focused on the intrinsic physical differences between the feed line and the patch antenna which can be postulated by the succeeding points which state that: 1) only the quasi-TEM wave is assumed to propagate along the uniform microstrip line; the feed line can, therefore, be conceptually evaluated by a static model and 2) only the structure discontinuities of the patch are responsible for all of the unbounded physical effects such as radiation and surface wave, so that the patch has to be dynamically modeled. With regard to the computational issue in the MoM, a principle of image (which allows the basis function to be continuously expanded along the feed line) is applied to replace the effect of the electric wall such that the resulting model becomes a versatile procedure for evaluating the input impedance of the antenna from the calculated magnitude of the basis functions designated at the terminal.

In this paper, such a procedure will be extended to formulate a generalized network model to characterize unbounded multiport microstrip circuit through an explicit representation of its network parameters. To do so, a delta-gap voltage source backed by the vertical electric wall is introduced to terminate each port that is externally connected with the microstrip circuit at an appropriate position. To apply the MoM, the current density flowing along the feed lines is deliberately expanded in terms of a linear combination of subsectional basis functions and their images which account for the effect of the local electrical wall. As such, the impedance matrix of the complete circuit can be explicitly derived from a matrix transformation. In addition, the choice of the open dyadic Green function allows to model unbounded physical effects generated by an open microstrip discontinuity.

This paper is organized as follows. In Section II, a delta-gap voltage source is introduced over the infinitesimally small gap between the perfect electric wall and the microstrip line. Then, the electric wall terminated multiport circuit is transformed into its open counterpart by separately handling the current density and the conductor surface of the feed line, where the image concept is used to remove the electric wall. In Section III, a MoM-based technique is applied to the numerical handling of the multiport circuit such that a systematic integral equation can be built for the solution of the unknown current density. In Section IV, the network parameters with reference to the terminals are explicitly deduced by a matrix transformation of impedance submatrices, which are related to the multiport feed lines and microstrip circuit, respectively. To demonstrate the usefulness of the proposed approach, a number of numerical and experimental results for the multiport circuit are presented in Section V which discusses the frequency-dependent characteristics of a two-port parallel-line bandpass filter and a four-port branch-line coupler.

II. Models of Generalized Port and Feed Line

It is known that the network parameters, namely, the admittance matrices (Y) or the impedance matrices (Z), should explicitly be formulated for a multiport circuit such that design and optimization of its electrical performance can be made in a deterministic manner. The key to a successful characterization of such a complex multiport geometry heavily depends on the selected strategy for modeling the related ports and feed lines. Thereafter, the network parameters can be derived from the calculated equivalent current and voltage located at each port terminal. To simplify the following consideration of analysis, the complete circuit can be divided into two distinct parts: microstrip discontinuity and circuit (the core part) to which the physical effects are attributed and an uniform microstrip line having an electrically thin dielectric substrate, where a quasi-TEM mode propagation can be postulated even if a dispersive mode can be used in the case of a multilayered structure.

To begin with the following analysis, we introduce a delta-gap voltage source backed by a vertically positioned electric wall at each port terminal which effectively simulates the

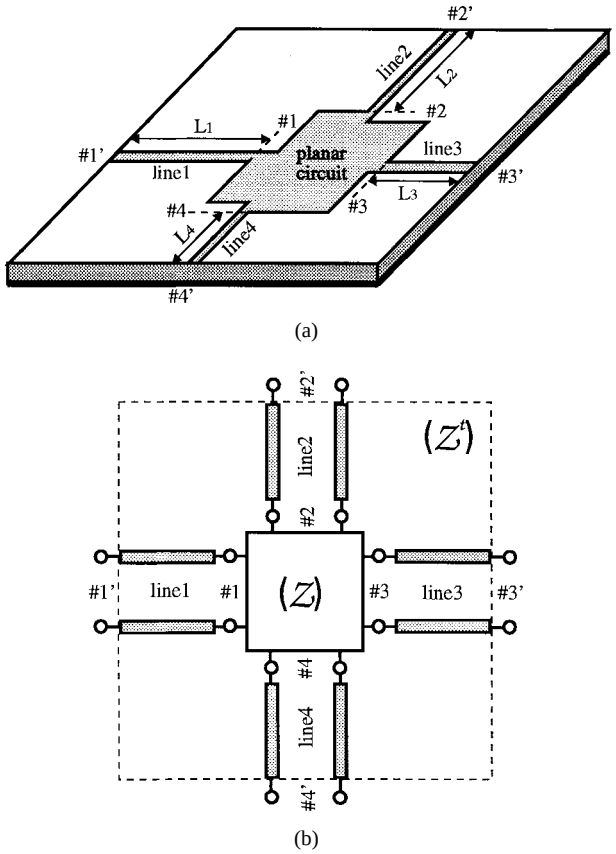

Fig. 1. A generalized unbounded four-port microstrip circuit. (a) Geometrical representation and (b) equivalent network.

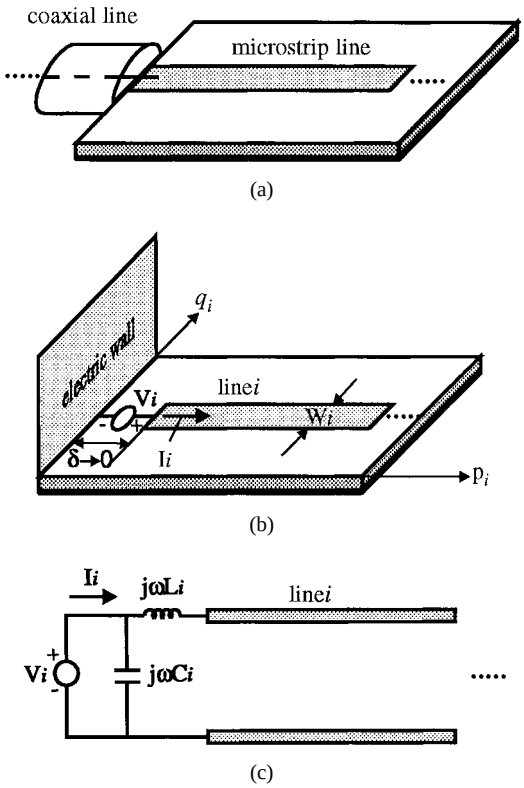

Fig. 2. The physical model of a generalized uniform feed line. (a) The transition from a coaxial line to a microstrip line. (b) The excitation mechanism of a delta-gap voltage source. (c) The equivalent circuit.

feeding mechanism between the microstrip line and coaxial-line probe [7], [21]. From the viewpoint of circuit, such a delta-gap voltage may be considered as the related terminal voltage while the total current flowing over the strip conductor located at the electric wall can be considered as the terminal current. To better illustrate the problem and its solution to be developed, a four-port microstrip circuit with arbitrarily shaped discontinuity is presented as an example, shown in Fig. 1(a), where each feed line is physically terminated by a delta-gap voltage source that is backed by a vertical electric wall. Fig. 1(b) shows its corresponding equivalent circuit network, for which the parameters such as impedance and admittance can be uniquely defined by the terminal voltage and current at each port.

Fig. 2(a) depicts the geometry of a generalized transition between the coaxial-line probe and the microstrip line. With reference to the topology of its structure, the excitation mechanism can be well described by the above-discussed delta-gap voltage V_i, as shown in Fig. 2(b). In the dynamic modeling, this voltage source should act as a mode launcher, as sketched in Fig. 2(b), to provide an incident electric field $\vec{E}_i^{\text{inc}}$ at ith port that can simply be described by

$$\vec{E}_i^{\text{inc}}(\vec{r}) = \vec{p}_i \cdot V_i \cdot \delta(p_i), \qquad q_i \in W_i \tag{1}$$

where p_i and q_i refer to two axis variables along the longitudinal and transversal directions on the feed line of ith port, respectively. Strictly speaking, the equivalent circuit of a port terminal should be modeled by a complete Y- or Z-parameter matrix, which is frequency-dependent. At low frequency, it may be suitably perceived as a static circuit composed of a parasitic shunt capacitance and a parasitic series inductance, as shown in Fig. 2(c). Nevertheless, the extremely small reactance makes it possible to completely ignore its influence under the condition of the electrically thin substrate.

To model the unbounded multiport microstrip circuit as shown in Fig. 1(a), an electric-field integral equation (EFIE) governing the total current density ($\vec{J}$) can be established on the conductor surface that includes each uniform feed line and the microstrip discontinuity. This is usually done by applying the Pocklington's integral equation and by imposing the boundary condition that invokes the vanishing of the total tangential electric field on the conductor surface. With the two distinct parts in mind, we can formulate the EFIE for a multiport circuit with M-ports such that

$$\vec{E}_i^{\text{inc}}(\vec{r}) + \sum_{j=1}^{M} \int_{\text{line}(j)} \overline{\overline{G}}_j(\vec{r}/\vec{r}_s) \cdot \vec{J}_j(\vec{r}_s)\, dS_s + \int_{\text{circuit}} \overline{\overline{G}}(\vec{r}/\vec{r}_s) \cdot \vec{J}(\vec{r}_s)\, dS_s = 0 \tag{2}$$

where $\overline{\overline{G}}(\vec{r}/\vec{r}_s)$ denotes the characteristic dyadic Green's function of the unbounded layered structure while $\overline{\overline{G}}_j(\vec{r}/\vec{r}_s)$ represents the local one associated with jth feed line ($j = 1, 2, \cdots, M$) which is terminated by the defined electric wall, as shown in Fig. 2. Using the image principle, the local dyadic Green's function can be expressed in terms of a simple linear superposition of $\overline{\overline{G}}(\vec{r}/\vec{r}_s)$ and its image counterpart

$\overline{\overline{G}}(\vec{r}/(\vec{r}_j - \vec{r}_s))$:

$$\overline{\overline{G}}_j(\vec{r}/\vec{r}_s) = \overline{\overline{G}}(\vec{r}/\vec{r}_s) + \overline{\overline{G}}[\vec{r}/(\vec{r}_j - \vec{r}_s)], \qquad \vec{r}_s \in j\text{th port}. \tag{3}$$

The second term of (3) introduced by the image principal can be perceived as a fictional current density $\vec{J}_j(\vec{r}_j - \vec{r}_s)$ appearing on the symmetrical side of $\vec{J}_j(\vec{r}_s)$ with reference to the jth electric wall $\vec{r}_j$, so that a generalized integral equation for a unbounded multiport circuit can be developed in the following form of a dyadic Green's function model:

$$\vec{E}_i^{\text{inc}}(\vec{r}) + \sum_{j=1}^{M} \int_{\text{line}(j)} \overline{\overline{G}}(\vec{r}/\vec{r}_s) \cdot [\vec{J}_j(\vec{r}_s) + \vec{J}_j(\vec{r}_j - \vec{r}_s)]\, dS_s + \int_{\text{circuit}} \overline{\overline{G}}(\vec{r}/\vec{r}_s) \cdot \vec{J}(\vec{r}_s)\, dS_s = 0. \tag{4}$$

The proposed integral equation (4) points to the use of the delta-gap voltage model and the partition of the complete multiport into the two distinct parts. Under the framework of the MoM, the vector function of current density over the conductor surface $\vec{J}(\vec{r}_s)$ is expanded into a set of subsectional basis functions. In this paper, these basis functions are composed of piecewise sinusoidal (PWS) functions in the longitudinal direction and pulse functions in the transversal direction. The condition of the quasi-TEM mode propagation leads to the only longitudinal component $\vec{q}_j J_j(p_j, q_j)$ that exists on the feed lines with a local coordinate (p_j, q_j) for jth port, as shown in Fig. 2(b). To simplify description of the following analysis, the model of feed line and port will be defined in a rectangular coordinate (x, z), as indicated in Fig. 3.

The actual existence of the electric wall at the terminal point ($z = 0$) under the original model of the port, as shown in Fig. 3(a), requires that the current density $J_z(x, z)$ be expanded via a complete set of PWS functions $J_{zm}(x, z)$, that should include a half-PWS term J_{z0} located at the terminal. Therefore, it is imperative to reflect this consideration in handling of the subsectional basis functions when the MoM is applied for simulation of the open environment. Similar to the above described procedure, the complete basis functions of current $J_{zbm}(x, z)$ should be made up of two terms, namely, the expanded basis function $J_{zm}(x, z)$ and its image function $J_{zm}(x, -z)$ at the local coordinate, as defined in Fig. 3(a) and Fig. 3(b) as follows:

$$J_{zbm}(x, z) = J_{zm}(x, z) + J_{zm}(x, -z), \qquad m = 0, 1, \cdots, M. \tag{5}$$

Likewise, (5) of the basis function that governs the current density flowing over the feed line completely takes into account the effect of the electric wall as the two sets of expanded function profiles are symmetrical at the two sides of the port terminal where the impressed delta-gap voltage source is located. Thus, the total current density $J_z(x, z)$ having a unknown magnitude I_j at the port of a feed line becomes

$$J_z(x, z) = I_j J_{z0}(x, z) + \sum_{j=1}^{M} I_j \cdot [J_{zj}(x, z) + J_{z(-j)}(x, z)]. \tag{6}$$

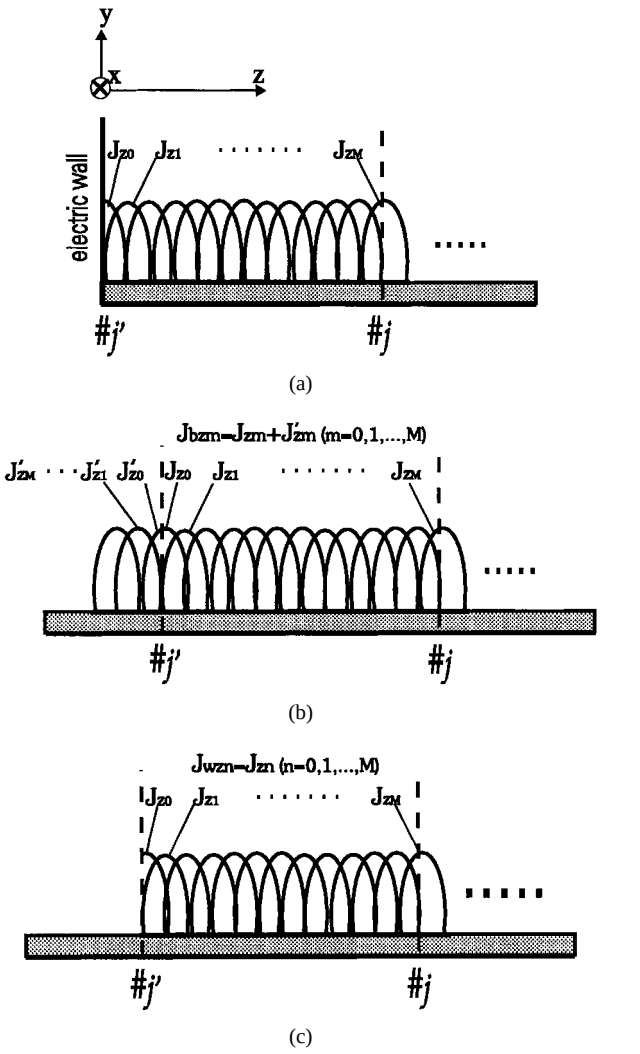

Fig. 3. The mathematical treatment of a uniform feed line backed by a vertically electric wall using the moment method. (a) The choice of current expansion functions for the prototype structure in Fig. 2(b). (b) and (c) The distinct choice of basis functions and weighting functions in the numerical procedure.

Subsequently, a set of weighting functions are to be selected for solving the integral equation (4) using the usual procedure of the MoM, which should reinforce the boundary condition on the conductor surface. Different from the simulation of the current density whose effective domain (by equivalence) was stretched to the other side of the port terminal, these weighting functions have to be defined in the physical domain of the feed line. They are formulated by a set of PWS functions including a half term of the terminal location, as shown in Fig. 3(c), which are completely identical with the expanded functions illustrated in Fig. 3(a).

So far, described is a procedure of transforming an infinitely long feed line into a finite one for the MoM simulation of a unbounded multiport circuit. It is also shown how to define the basis and weighting functions. This proposed port model spells out two principal advantages: it provides a theoretical platform for the use of circuit parameters in the explicit modeling of multiport microstrip circuit and it leads to an accurate model that can include all of the physical effects taking place in an open and layered structure.

III. Formulation for the MoM

In the previous section, we have formulated an EFIE in (4) for modeling of an open microstrip circuit where the complete multiport circuit is divided into two regions, namely, the uniform feed lines and the microstrip circuit. It is known that a generalized feed line can be modeled by using two different sets of functions (basis and weighting terms) for proceeding with the MoM. The microstrip circuit region will also be discretized by a number of rectangular meshes similar to those defined for the feed lines. For each mesh, both basis and weighting functions are selected by simply multiplying a PWS function along the longitudinal direction and a pulse function in the transverse direction. Since fields over the circuit region are not affected by the electric walls located at the terminal of each uniform feed line that is supposed to be far away from the designated circuit, the expansion of current density over the circuit region will not resort to any additional image term.

To be concise, a four-port structure defined in a rectangular coordinate will be considered in the following development. Through a Fourier transform, (4) can be formulated into the form of an algebraic spectral-domain convolution integral as follows:

$$\sum_{j=1}^{M} \tilde{\vec{E}}_j^{\text{inc}}(\alpha,\beta) + \sum_{j=1}^{M} \tilde{\overline{\overline{G}}}(\alpha,\beta)\cdot\left[\tilde{\vec{J}}_j(\alpha,\beta) + \tilde{\vec{J}}'_j(\alpha,\beta)\right] + \tilde{\overline{\overline{G}}}(\alpha,\beta)\cdot\tilde{\vec{J}}(\alpha,\beta) = 0 \tag{7}$$

where α, β are two spectral domain variables corresponding to their space-domain counterparts x, z. In (7), the spectral-term script is applied to all related variables and functions. The current densities which are defined in each individual local coordinate for the two distinct regions are, for example, transformed into

$$\tilde{\vec{J}}_j(\alpha,\beta) = \sum_{m=0}^{M_j} I_{jm}\tilde{\vec{J}}_{jm}(\alpha,\beta) = \sum_{m=0}^{M_j} I_{jm}\begin{cases}\hat{x}\tilde{J}_{xjm}(\alpha,\beta), & \vec{J}_j = \hat{x}J_j\\ \hat{z}\tilde{J}_{zjm}(\alpha,\beta), & \vec{J}_j = \hat{z}J_j\end{cases} \tag{8a}$$

$$\tilde{\vec{J}}'_j(\alpha,\beta) = \sum_{m=0}^{M_j} I_{jm}\tilde{\vec{J}}'_{jm}(\alpha,\beta) = \sum_{m=0}^{M_j} I_{jm}\begin{cases}\hat{x}\tilde{J}_{xjm}(-\alpha,\beta), & \vec{J}_j = \hat{x}J_j\\ \hat{z}\tilde{J}_{zjm}(\alpha,-\beta), & \vec{J}_j = \hat{z}J_j\end{cases} \tag{8b}$$

$$\tilde{\vec{J}}(\alpha,\beta) = \sum_m\sum_n I_{xmn}\hat{x}\tilde{J}_{xmn}(\alpha,\beta) + \sum_n\sum_m I_{znm}\hat{z}\tilde{J}_{znm}(\alpha,\beta) \tag{8c}$$

in which I_{jm} is the magnitude of basis functions in the feed line region while I_{xmn} and I_{zmn} are those of x- and z-axis basis functions in the circuit region, respectively. The subscript jm refers to the mth mesh in the local coordinate for the jth feed line. The comparison of (8a) with (8b) suggests that the image term $\tilde{\vec{J}}'_{jm}(\alpha,\beta)$ in the spectral domain can be interpreted as an accompanied term of its original counterpart with a negative symbol attached to the axial variable. As a result, the current densities flowing on each feed line can be mathematically expressed in terms of a linear combination of two interrelated functions $\tilde{\vec{J}}_{jm}(\alpha,\beta)$ and $\tilde{\vec{J}}'_{jm}(\alpha,\beta)$, whereas two independent sets of functions, namely, $\hat{x}\tilde{J}_{xmn}(\alpha,\beta)$ and $\hat{z}\tilde{J}_{znm}(\alpha,\beta)$, are imposed on the circuit region. Thus, two typical expanded functions for the two regions can be formulated as shown in (9a) and (9b), at the bottom of the page, where $\tilde{J}_{xjm}(\beta)$ and $\tilde{J}_{xmn}(\beta)$ are spectral terms of the pulse functions for the feed line and the microstrip circuit, respectively. The symbol k_e is an arbitrary constant in the PWS functions which is selected as the precalculated phase constant of a dominant mode propagating along one of the feed lines. The variables x_{jm}, x_{mn}, and Δx_{jm}, Δx_{mn} refer, respectively, to the position and the size of the abscissa (x) mesh located at the mth point of the jth feed line, and similarly the mth point along x-axis and nth along z-axis for the circuit region. Through the right-hand side (RHS) of (9a), it can be found that the spectral-domain formulation of the x-oriented basis functions is split into two different forms: one represents an impressed half-sinusoidal basis function located at the original point of the local coordinate ($m = 0$) while the other stands for the entire domain of the feed lines, except the original point ($m \neq 0$).

With consideration of the above-mentioned factors on the choice of the weighting functions $\vec{J}_w(\alpha,\beta)$, we apply the standard procedure of the MoM to (7) which leads to a spectral domain integral equation in the form of a double integration. This integral equation can be further arranged in the source-type form by relocating the impressed field's term to the RHS such as

$$\int_{-\infty}^{+\infty}\int_{-\infty}^{+\infty} \tilde{\vec{J}}_w(\alpha,\beta)\cdot\tilde{\overline{\overline{G}}}(\alpha,\beta)\cdot\left\{\sum_{j=1}^{M}\left[\tilde{\vec{J}}_j(\alpha,\beta)+\tilde{\vec{J}}'_j(\alpha,\beta)\right]+\tilde{\vec{J}}(\alpha,\beta)\right\}d\alpha\,d\beta = -\int_{-\infty}^{+\infty}\int_{-\infty}^{+\infty}\tilde{\vec{J}}_w(\alpha,\beta)\cdot\sum_{j=1}^{M}\tilde{\vec{E}}_j^{\text{inc}}(\alpha,\beta)\,d\alpha\,d\beta. \tag{10}$$

$$\tilde{J}_{xjm}(\pm\alpha,\beta) = \frac{\tilde{J}_{xjm}(\beta)}{\sin(k_e\Delta x_{jm})(\alpha^2-k_e^2)}\cdot\begin{cases}k_e\cos(k_e\Delta x_{jm})\pm j\alpha\sin(k_e\Delta x_{jm}) - k_e e^{\pm j\alpha\Delta x_{jm}}, & m=0\\ 2k_e[\cos(k_e\Delta x_{jm})-\cos(\alpha\Delta x_{jm})]\cdot e^{\pm j\alpha x_{jm}}, & m\neq 0\end{cases} \tag{9a}$$

$$\tilde{J}_{xmn}(\alpha,\beta) = \frac{\tilde{J}_{xmn}(\beta)}{\sin(k_e\Delta x_{mn})(\alpha^2-k_e^2)}\cdot 2k_e[\cos(k_e\Delta x_{mn})-\cos(\alpha\Delta x_{mn})]\cdot e^{j\alpha x_{mn}} \tag{9b}$$

Considering the inner product of the resulting integral equation (10), the weighting function takes the conjugated form of its counterpart of the basis function, which leads to negative variables in the spectral-domain formulation as shown in (11), at the bottom of the page.

The generality of the unbounded dyadic Green's function allows one to extract all of possible physical effects from the double infinite integrals in (10) such as the space-wave radiation and the surface-wave leakage, as well as all of the modes guided along each feed line [13]. The tedious and troublesome double integration over the infinite range requires that the rectangular coordinate be transformed into its polar counterpart in the spectral domain such that evaluation of these effects can be greatly simplified and also more accurate. The effect of the space wave can be precisely calculated numerically from an integration over the range of $(\alpha^2+\beta^2) \leq k_0^2$, while the surface wave effect can be analytically obtained by the residue values of the poles that are located in the range of $k_0^2 < (\alpha^2+\beta^2) < \varepsilon_r k_0^2$.

It is known that the uniform feed lines allow only the propagation of the quasi-TEM mode and higher order modes should be completely vanishing at a location far away from the microstrip circuit (discontinuity) while the space wave and the surface wave are excited at or near the discontinuity, which propagate upward into space and outbound from the discontinuity along the dielectric layer. In fact, the so-called excitation mechanism is a mathematical framework that effectively simulates the propagation of the dominant mode along the feed line. On the left-hand side (LHS) of (10), the integral associated with the first two terms essentially contributes to the effects of propagating modes along the feed line while the last term is related to the effects of space and surface waves as well as all of possible propagating modes. The integral related to the source term on the RHS of (10) completely describes the effect of the dominant mode propagation on the feed line. Similar to other models [1], [2], all of the physical effects can be accurately taken into account by the characteristic integral equation (10).

Fig. 4 shows different arrangement of the basis functions and weighting functions for the four-port microstrip structure. The relevant domain of each feed line as indicated in Fig. 4(a) is locally stretched outside the port terminal to represent the image current flowing along the reverse side such that the electric wall is effectively replaced. The complete symmetrical domain is discretized by rectangular meshes and the delta-gap voltage sources are impressed at each port terminal that are related to the tangential electric field E_i. The feed lines may require a transverse discretization with more than one mesh (first and third ports, for example) to cope with different strip widths that is a practical situation. In this case, the impressed electric fields (delta-gap voltage source) with identical magnitude defined for these transverse meshes are imposed. Fig. 4(b) demonstrates the choice of the corresponding weighting functions for the four-port which is only related to the physical feed lines. Basically, the whole procedure is quite similar to the Galerkin technique in the spectral domain, except that the basis functions and the weighting functions are formulated differently on the feed lines.

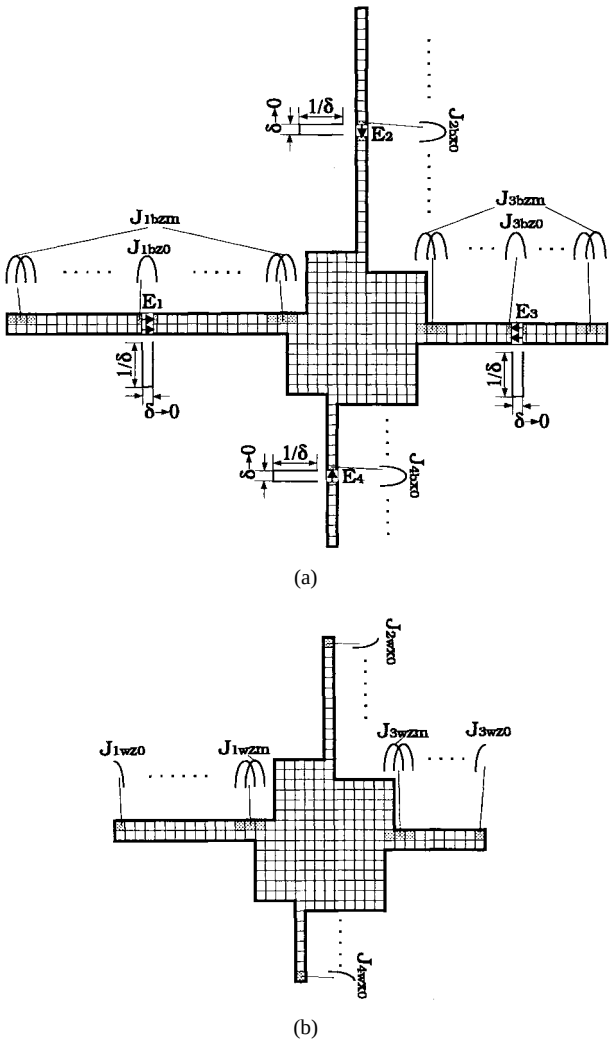

Fig. 4. The systematically schematic description for an arbitrary open four-port microstrip circuit. (a) The arrangement of basis functions and local delta-gap voltages. (b) The arrangement of weighting functions.

IV. Matrix Equation for Explicit Network Parameters

The complex physical effects are implicitly determined by solving (10) for a particular unbounded multiport circuit that may have an arbitrary shape of the topology. Choosing the same number of the weighting functions as that of the basis functions, we are able to derive a source-type matrix equation

$$\tilde{\vec{J}}_w(\alpha,\beta) = \begin{cases} \tilde{\vec{J}}_{jm'}(-\alpha,-\beta), \\ \tilde{\vec{J}}_{xm'n'}(-\alpha,-\beta), \\ \tilde{\vec{J}}_{zn'm'}(-\alpha,-\beta), \end{cases} \quad \begin{matrix} j=1,\cdots,M;\ m'=0,1,\cdots,M_j \\ m'=1,2,\cdots;\ n'=1,2,\cdots \end{matrix} \tag{11}$$

that clearly points to the excitation and its related response, such that

$$\begin{bmatrix} (\mathcal{Z}^{pp}) & (\mathcal{Z}^{pc_x}) & (\mathcal{Z}^{pc_z}) \\ (\mathcal{Z}^{c_xp}) & (\mathcal{Z}^{c_xc_x}) & (\mathcal{Z}^{c_xc_z}) \\ (\mathcal{Z}^{c_zp}) & (\mathcal{Z}^{c_zc_x}) & (\mathcal{Z}^{c_zc_z}) \end{bmatrix} \cdot \begin{bmatrix} (I^p) \\ (I^{c_x}) \\ (I^{c_z}) \end{bmatrix} = \begin{bmatrix} (\mathcal{V}^p) \\ (\mathcal{O}) \\ (\mathcal{O}) \end{bmatrix} \quad (12)$$

where the superscripts p, c_x, c_z stand for physical orientation of the basis functions and the weighting functions defined along the uniform feed lines and the port terminal as well as over the microstrip circuits (x- and z-axes). Each submatrice $(\mathcal{Z}^{ab})(a, b = p, c_x, c_z)$ describes the coupling (interaction) between two orientations of discretized field functions. The submatrices $(I^a)(a = p, c_x, c_z)$ are related to magnitudes of the basis functions for the current-density meshes designated over the conductor surface. On the other hand, the submatrice $(\mathcal{V}^p)$ refers to magnitudes of each voltage source, and it is expressed in terms of a spectral-domain convolution of the impressed electric fields and the weighting functions.

Without loss of generality, we can assume the feed lines to be arranged far away from each other so that the submatrices of impedance associated with each feed line can be separately formulated. In this way, the explicit network parameters of a unbounded generalized multiport microstrip circuit can be derived from the extraction of such a characteristic matrix, as in (12). In the calculation, the coupling effect between the fields of the port terminal and the microstrip circuit is reinforced to be negligible such that the possible influence of the electric wall on the physical waves attributed by the microstrip discontinuity can be effectively avoided (at least minimized). According to (10), the matrix elements in (12) can be formulated in the spectral domain as shown in (13a)–(13d), at the bottom of the page, in which the subscripts im and jn number the position of the basis functions and the weighting functions defined at each local coordinate of the feed lines while the subscripts $\mathtt{kl}$ and $\mathtt{mn}$ also indicate the position, but in a global rectangular coordinate. The symbols k and l point to the flowing directions of the current defined over the microstrip circuit for both basis and weighting functions. The calculation of these double integrals should be carried out in the polar coordinate, as suggested previously.

On the basis of physical phenomena possibly appearing in a multiport microstrip structure, it is known that the submatrices of impedance governed by (12) can be classified by considering the above mentioned two regions (multiport and circuit). To derive its network representation, the multiport should be further divided into the port terminals and the uniform feed lines. To simplify description of the matrix equation, on the other hand, four groups of submatrices in (12) that are related to the x- and z-axes currents flowing over the microstrip circuit are put together in a new matrix equation (14), which is in line with the explicit formulation of network parameters. In addition, the submatrices related to the source term at the RHS of (12) can be also arranged to formulate a voltage submatrix associated with all of the port terminals

$$\begin{bmatrix} (\mathcal{Z}^{tt}) & (\mathcal{Z}^{tf}) & (\mathcal{O}) \\ (\mathcal{Z}^{ft}) & (\mathcal{Z}^{ff}) & (\mathcal{Z}^{fc}) \\ (\mathcal{O}) & (\mathcal{Z}^{cf}) & (\mathcal{Z}^{cc}) \end{bmatrix} \cdot \begin{bmatrix} (I^t) \\ (I^f) \\ (I^c) \end{bmatrix} = \begin{bmatrix} (\mathcal{V}^t) \\ (\mathcal{O}) \\ (\mathcal{O}) \end{bmatrix} \quad (14)$$

in which (I^t) and $(\mathcal{V}^t)$ are two groups of the column submatrices associated with the magnitudes of the basis functions and the impressed voltages. The superscripts t, f, and c refer to port terminal, uniform feed line, and circuit, respectively. In this procedure, the feed lines are discretized with only one mesh in the transverse direction, and the elements in the two submatrices are equivalent to the terminal current and voltage. However, as explained in Section III, it is desirable to use more than one mesh for the feed lines for practical considerations. Therefore, in a mathematical model the elements in these two column submatrices should be considered as the groups (submatrices) to accommodate this factor. To do so, such submatrices are expressed by symbols having the dash line on the top, and can be written as the following vectors

$$Z^{pp}_{imjn} = -4\pi^2 \cdot \begin{cases} \displaystyle\int_{-\infty}^{+\infty}\int_{-\infty}^{+\infty} \tilde{\vec{J}}_{im}(-\alpha, -\beta) \cdot \tilde{\bar{\bar{G}}}(\alpha, \beta) \\ \quad \cdot \left[\tilde{\vec{J}}_{j_n}(\alpha, \beta) + \tilde{\vec{J}}'_{j_n}(\alpha, \beta)\right] d\alpha\, d\beta & (i = j) \\ 0 & (i \neq j) \end{cases} \quad (13a)$$

$$Z^{pc_l}_{im\mathtt{mn}} = -4\pi^2 \cdot \begin{cases} \displaystyle\int_{-\infty}^{+\infty}\int_{-\infty}^{+\infty} \tilde{\vec{J}}_{im}(-\alpha, -\beta) \cdot \tilde{\bar{\bar{G}}}(\alpha, \beta) & (l = x, z) \\ \quad \cdot \hat{l}\tilde{J}_{l\mathtt{mn}}(\alpha, \beta)\, d\alpha\, d\beta & (m \neq 0) \\ 0 & (m = 0) \end{cases} \quad (13b)$$

$$Z^{c_kp}_{\mathtt{kl}jn} = -4\pi^2 \cdot \begin{cases} \displaystyle\int_{-\infty}^{+\infty}\int_{-\infty}^{+\infty} \hat{k}\tilde{J}_{k\mathtt{kl}}(\alpha, \beta) \cdot \tilde{\bar{\bar{G}}}(\alpha, \beta) & (k = x, z) \\ \quad \cdot \left[\tilde{\vec{J}}_{jn}(\alpha, \beta) + \tilde{\vec{J}}'_{jn}(\alpha, \beta)\right] d\alpha\, d\beta & (n \neq 0) \\ 0 & (n = 0) \end{cases} \quad (13c)$$

$$Z^{c_kc_l}_{\mathtt{kl}m\mathtt{n}} = -4\pi^2 \cdot \int_{-\infty}^{+\infty}\int_{-\infty}^{+\infty} \hat{k}\tilde{J}_{k\mathtt{kl}}(\alpha, \beta) \cdot \tilde{\bar{\bar{G}}}(\alpha, \beta) \cdot \hat{l}\tilde{J}_{l\mathtt{mn}}(\alpha, \beta)\, d\alpha\, d\beta \qquad (k = x, z; l = x, z) \quad (13d)$$

(submatrices) for an M-port structure:

$$(\overline{I}^t) = \begin{bmatrix} \overline{I}_1^t \\ \overline{I}_2^t \\ \vdots \\ \overline{I}_M^t \end{bmatrix} \quad (\overline{V}^t) = \begin{bmatrix} \overline{V}_1^t \\ \overline{V}_2^t \\ \vdots \\ \overline{V}_M^t \end{bmatrix}. \tag{15}$$

Since the topology of the excitation model described in Fig. 2 can be basically viewed as an equivalent parallel circuit, we can easily deduce, through a simple matrix transform of (14), an explicit relationship between these two vectors such as

$$(\overline{\mathcal{Z}}^t)\,(\overline{I}^t) = (\overline{V}^t). \tag{16}$$

$(\overline{\mathcal{Z}}^t)$ is the terminal impedance matrix and can be defined by the following:

$$\begin{aligned}(\overline{\mathcal{Z}}^t) = {} & (\mathcal{Z}^{tt}) - (\mathcal{Z}^{tf}) \cdot (\mathcal{Z}^{ff})^{-1} \cdot (\mathcal{Z}^{ft}) + (\mathcal{Z}^{tf}) \\ & \cdot (\mathcal{Z}^{cf})^{-1} \cdot (\mathcal{Z}^{cc}) \cdot (\mathcal{Z}^{fc})^{-1} \cdot (\mathcal{Z}^{ft}).\end{aligned} \tag{17}$$

Now, the subsequent attention will be centered on how to extract the realistic terminal network parameters for the explicit modeling of an open multiport circuit as proposed in [19]. Immediately, the terminal admittance matrix $(\overline{\mathcal{Z}}^t)$ can be obtained by simply inverting it impedance counterpart $(\overline{\mathcal{Y}}^t)$, which can be formulated for the port-related submatrices

$$(\overline{\mathcal{Y}}^t) = (\overline{\mathcal{Z}}^t)^{-1} = \begin{bmatrix} (\overline{\mathcal{Y}}_{11}^t) & \cdots & (\overline{\mathcal{Y}}_{1\mathcal{M}}^t) \\ \vdots & \ddots & \vdots \\ (\overline{\mathcal{Y}}_{\mathcal{M}1}^t) & \cdots & (\overline{\mathcal{Y}}_{\mathcal{M}\mathcal{M}}^t) \end{bmatrix}. \tag{18}$$

Then, the realistic terminal admittance matrix for the circuit model can be designated as a matrix relationship between the physical terminal currents and voltages

$$(\mathcal{Y}^t) \cdot (V^t) = (I^t) \tag{19}$$

and the matrix element $\mathcal{Y}_{ij}^t$ in $(\mathcal{Y}^t)$ can be derived from its corresponding submatrice, considering the fact that the transverse meshes in a port terminal can be modeled and identified by its physical parallel circuit. Therefore, we have

$$\mathcal{Y}_{ij}^t = (U)_{m_i \times m_i} \cdot (\overline{\mathcal{Y}}_{ij}^t)_{m_i \times m_j} \cdot (U)_{m_j \times m_j} \tag{20}$$

where the subscripts m_i and m_j refer to the numbers of the transverse meshes in the ith and jth port terminals, respectively, and (U) is the unit matrix.

Using the standard network theory, we can analytically deduce the related impedance parameters and the scattering parameters. The former $(\mathcal{Z}^t)$ is directly equal to the inversion of $(\mathcal{Y}^t)$ and the latter $(\mathcal{S}^t)$ is calculated through $(\mathcal{Z}^t)$

$$(\mathcal{S}^t) = (U) - 2\left[(W^f)^{-1} \cdot (\mathcal{Z}^t) \cdot (W^f)^{-1} + (U)\right]^{-1} \tag{21}$$

where (W^f) is a diagonal impedance matrix that incorporate the characteristic impedance of the related uniform feed lines and can be determined by

$$(W^f) = \begin{bmatrix} \sqrt{Z_{O1}} & \cdots & 0 \\ \vdots & \ddots & \vdots \\ 0 & \cdots & \sqrt{Z_{OM}} \end{bmatrix}. \tag{22}$$

The scattering parameters defined at a particular designated reference plane for each feed line can be obtained by considering the relative electrical length of the port measured from its reference plane. The complete scattering matrix for the unbounded multiport circuit of interest can be obtained by the following equation:

$$(\mathcal{S}) = (V^f) \cdot (\mathcal{S}^t) \cdot (V^f) \tag{23}$$

where (V^f) is a diagonal phase matrix which is defined by

$$(V^f) = \begin{bmatrix} e^{j\theta_1} & \cdots & 0 \\ \vdots & \ddots & \vdots \\ 0 & \cdots & e^{j\theta_M} \end{bmatrix}. \tag{24}$$

Of course, the alternative representation of the network can be used, such as $(\mathcal{Z})$ and $(\mathcal{Y})$. They can be derived by applying the network theory and matrix transform. The complete impedance matrix, for example, should become

$$(\mathcal{Z}) = (W^f) \cdot \left\{2[(U) - (\mathcal{S})]^{-1} - (U)\right\} \cdot (W^f). \tag{25}$$

V. Results and Discussion

Generally speaking, the choice of network parameters such as (S) and (Z) or (Y) depends on the application aspect of a particular multiport circuit. The above characteristic matrix of the network parameter can be used to model, design, and optimize a unbounded multiport circuit having arbitrary shape, clearly laying a ground for a field–theoretical computer-aided design (CAD). The proposed modeling technique can be used to accurately predict the unbounded effects such as the radiation loss and leakage problems of planar integrated circuits such as miniaturized (hybrid) microwave integrated circuits (M(H)MIC's) when stringent design issues should be addressed at high frequencies for commercial applications that are readily moving into millimeter-wave range. The network parameters are extremely useful for high-frequency multilayered passive and active circuit design such as impedance matching network, amplifier, mixer, diplexer, and so forth. From the circuit point of view, an open multiport circuit can be represented by a lossy network with a set of frequency-dependent equivalent circuit parameters. These circuit parameters may be useful for high-speed interconnects of multiple lines and multilayered packaging design.

On the other hand, direct evaluation of the radiation efficiency and resonance characteristics of a radiating structure always presents a very important design issue since the planar radiating structure has relatively narrow bandwidth that has to be precisely predicted from such a field-based model. Possible arbitrary shape of the radiating structure can be accurately modeled for some special applications. In addition, the leakage effect existing in a layered planar structure may be deliberately suppressed for circuit application, and also may be used to design a leaky-wave antenna for compact and narrow beamwidth applications. In addition, this modeling technique can be used to design a multilayered feeding network considering the load and proximity effect of radiating structure for passive and active antenna applications.

As the first example, a two-port open parallel coupled-line bandpass filter is depicted in Fig. 5 together with its theoretical

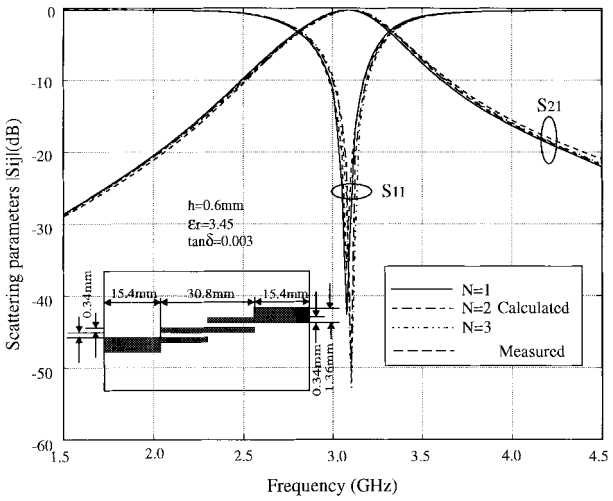

Fig. 5. Simulated and measured scattering parameters of a parallel coupled-line bandpass filter.

and experimental results. The strip width of the two feed lines (the input and output ports of the filter) are adjusted by the use of a 2-D MoM such that 50-Ω matching with the external connecting lines can be made. A narrow width of the coupled lines compared to that of the feed lines is selected to achieve a strong coupling between two adjacent parallel lines. The total discontinuity consists of two parts: the coupled lines and the step transitions.

In our modeling, the feed lines are discretized with more than one mesh along the linewidth, and they are modeled by using the matrix equation given in (17)–(25). In this case, three mesh schemes are made to effectively discretize the complete conductor shape. In this way, a convergence analysis is made for which $\Delta x = 0.11$, 0.17, and 0.34 mm and $\Delta z = 2.05$, 3.08, and 6.16 mm are used for the three discretization schemes, $N = 3$, 2, 1, related to the transverse and longitudinal directions, respectively. It should be noted that the transverse basis functions next to the step transitions should be chosen to reflect the influence of higher order modes. Under these considerations, the scattering parameters of the filter are simulated, which are very well compared with the experimental results. In addition, the numerical stability and convergence behavior are very well observed in the figure. As shown in Fig. 5, the frequency shift of S_{11} among them is found to be less than 0.5%. In addition, the radiation loss of the filter is also calculated through the normalized power $\left(|S|_{11}^2 + |S|_{21}^2\right)$, and it is found to be less than 2.0% of the total injected power over the frequency range of interest.

To further demonstrate the usefulness of the proposed technique for unbounded multiport microstrip circuits, an open four-port branch-line microstrip coupler that was presented in [16] based on the FDTD method is considered for the last example of our simulation. Fig. 6(a) presents its layout whose strip widths—except two parallel lines connecting port-one and port-two, or port-three and port-four—are selected the same as those of [16] for the comparison purpose. Our intention is to make these two parallel lines variable such that electrical performance of the coupler can be visualized and high-quality coupler can be designed on the basis of the field–theoretical tool. Essentially, the length of the four branch lines is usually equal to a quarter-guided-wavelength that achieves 90° phase difference between port-three and port-four. To be consistent with the circuit topology, the size of a uniform mesh dimension is used with $\Delta x = \Delta z = 0.812$ mm, twice those used in [16], and the feed line between the terminal and reference positions is discretized by 4×12. First, (17) is used to obtain a 16×16 matrix elements of $(\mathcal{Z}^t)$ having a double spectral integration. Then, the admittance parameters $(\mathcal{Y}^t)$ defined at the four-port terminals are simply determined by multiplying 4×4 matrices in (21). In this way, the scattering parameter matrix (S^t) of the coupler can be obtained from a simple matrix calculation governed by (21) and (23).

Fig. 6(b) provides the modeled frequency response of $|S_{31}|$ and $|S_{41}|$ for three different strip widths W, defined in Fig. 6(a). It is observed that in the proximity at $f = 6.0$ GHz, the increase of W brings $|S_{31}|$ to shift toward lower coupling and $|S_{41}|$ higher coupling. This may yield unbalanced situations. The coupling coefficients $|S_{31}|$ and $|S_{41}|$ are found to be approximately -3 dB when $W = 4.06$ mm. It can be well explained from the design point of view that the ratio of the characteristic impedance of the transverse and longitudinal branch lines is extremely close to the theoretical optimum value of $\sqrt{2}$. The simulation results indicate that the electrical performance of the branch-line coupler is quite sensitive to the linewidth. Fig. 6(c) shows our simulation results together with the measurements and the numerical results obtained by the FDTD in [16] for the case of $W = 4.06$ mm. The comparison of these plotted curves indicates a very satisfactory agreement for the magnitude of all the four scattering parameters. In particular, our results predict very well the central frequency and bandwidth performance of the coupler compared to the FDTD simulations. In addition, the phase difference $\arg(S_{31}/S_{41})$ between port-three and port-four is given in Fig. 6(d) for three different linewidth (W). Once again, our results agree well with those of the FDTD and the measurements and they are more close to the measurements than the FDTD in the frequency bandwidth of interest. On the other hand, the phase difference is found to be stationary and it is equal to 90° around the central frequency point even if W is altered. Otherwise, the phase curves tend to be up-and-down over the frequency range. In addition, the radiation loss of the branch-line coupler is also calculated through our modeling technique for which there are no results available from other alternative techniques. These results plotted in Fig. 6(e) clearly indicate that the maximum of radiation loss appears over the effective frequency bandwidth. The maximum power loss of about 5.5% at the central operating frequency ($f = 6.3$ GHz) is observed although there is a minor shift of power loss response over frequency range for three different W's. This can be very well explained by the fact that the branch-line coupler can be regarded as a resonator-type microstrip ring antenna attached with the four feed lines. Moreover, the maximum possible radiation should take place only if the ring oscillates (becomes a resonator). Nevertheless, the curves of the radiation loss behave shapely for a narrow line ($W = 2.436$ mm), and

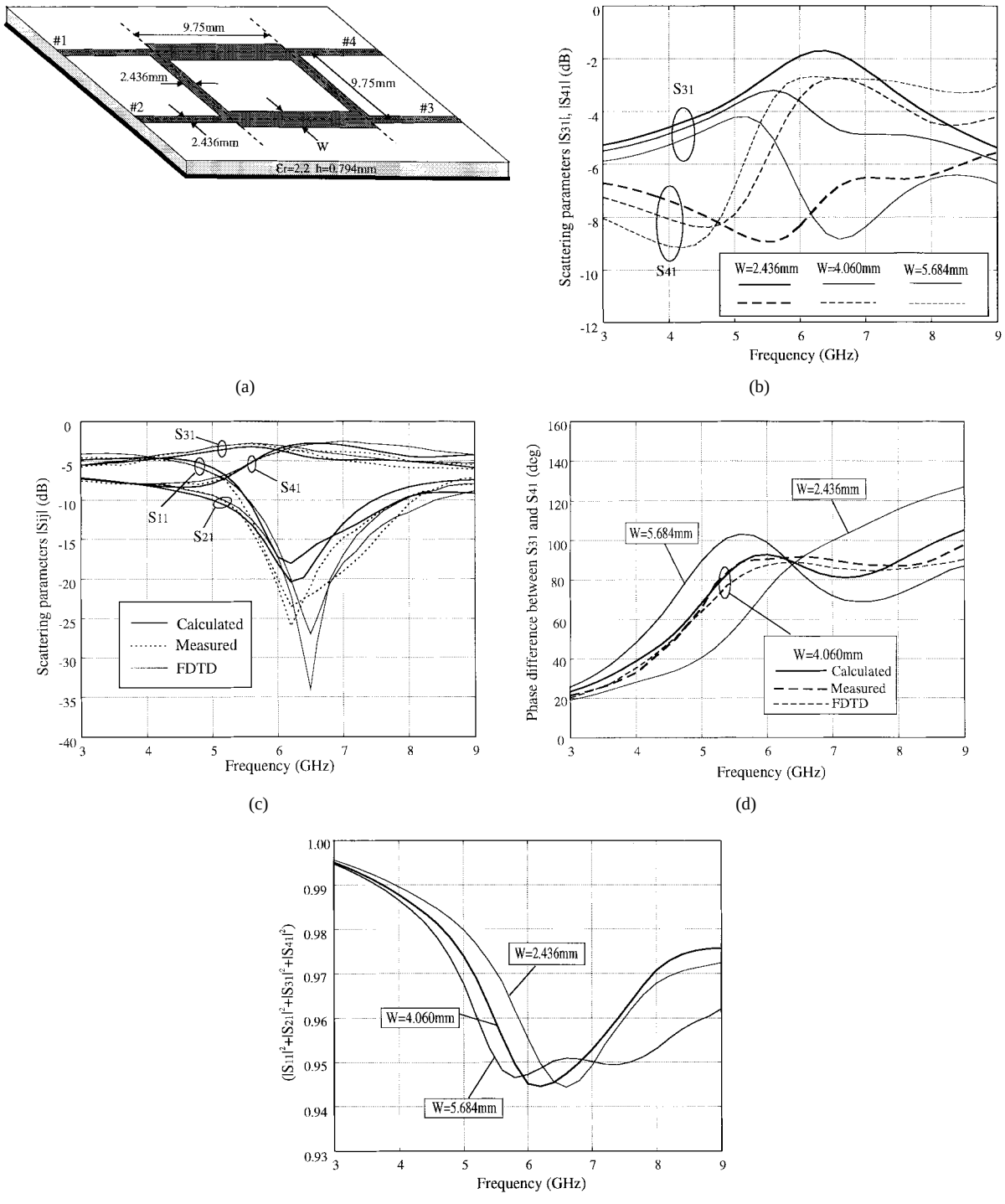

Fig. 6. Numerical modeling of an open four-port branch line microstrip coupler. (a) Its structural topology, (b) variation of simulated $|S_{31}|$ and $|S_{41}|$ as a function of the strip width W, (c) comparison with the measured and FDTD's results, (d) characteristics of phase difference $\arg(S_{31}/S_{41})$, and (e) simulated radiation losses as a function of frequency.

otherwise, the frequency response of the radiation loss tends to be flat over the effective bandwidth and also the radiation loss is slightly reduced in the case of a wide line ($W = 5.684$ mm).

VI. Conclusion

This paper presents a generalized framework using explicit network-parameters-based MoM for field–theoretical modeling and design of unbounded multiport microstrip circuits and antennas. A systematic study of the excitation mechanism is made for the explicit representation of network parameters when the MoM is applied. This paper presents a detailed procedure of how to set up a unified multiport impressed delta-gap source model and also how to partition a complete circuit into subregions under the MoM. It is demonstrated that a deterministic network parameter model can be established

so that the equivalent circuit model can be directly extracted from the moment-field model. In addition, the image principal is applied to the removal of the electric walls and, therefore, open environment can be effectively simulated for obtaining power radiation characteristics. Two multiport simulation examples presented in this paper that include experimental results and comparison with other available results indicate that a unified and efficient equivalent multiport circuit model can be obtained from the field–theoretical technique and can be used for precision design and optimization of circuits and antennas. Convergence analysis is also presented for the filter example, showing the numerical stability and convergence behavior. Performance analysis of open multiport examples suggests that accurate modeling be mandatory in accounting for any potential radiation loss and other physical effects.

ACKNOWLEDGMENT

One of the authors, L. Zhu, wishes to thank the Research and Development Laboratory of Matsushita-Kotobuki Electronics Industries, Ltd., Japan, for its technical support on the development of MoM-based software toward the design of planar antennas for wireless communications. The authors also would like to thank this paper's first reviewer for his valuable discussions on the numerical de-embedding techniques.

REFERENCES

[1] P. B. Katehi and N. G. Alexopoulos, "Frequency-dependent characteristics of microstrip discontinuities in millimeter-wave integrated circuits," *IEEE Trans. Microwave Theory Tech.*, vol. MTT-33, pp. 1029–1035, Oct. 1985.

[2] R. W. Jackson and D. M. Pozar, "Full-wave analysis of microstrip open-end and gap discontinuities," *IEEE Trans. Microwave Theory Tech.*, vol. MTT-33, pp. 1036–1042, Oct. 1985.

[3] R. H. Jansen, "The spectral-domain approach for microwave integrated circuits," *IEEE Trans. Microwave Theory Tech.*, vol. MTT-33, pp. 1043–1056, Oct. 1985.

[4] R. H. Jansen and W. Wertgen, "Modular source-type 3-D analysis of scattering parameters for general discontinuities, components and coupling effects in (M)MIC's," in *17th European Microwave Conf. Proc.*, Rome, Italy, Sept. 1987, pp. 427–432.

[5] J. R. Rautio and R. F. Harrington, "An electromagnetic time-harmonic analysis of shielded microstrip circuits," *IEEE Trans. Microwave Theory Tech.*, vol. MTT-35, pp. 726–730, Aug. 1987.

[6] H. Y. Yang and N. G. Alexopoulos, "Basic blocks for high frequency interconnects: Theory and experiment," *IEEE Trans. Microwave Theory Tech.*, vol. 36, pp. 1258–1264, Aug. 1988.

[7] L. P. Dunleavy and P. B. Katehi, "A generalized method for analyzing thin microstrip discontinuities," *IEEE Trans. Microwave Theory Tech.*, vol. 36, pp. 1758–1766, Dec. 1988.

[8] J. R. Mosig, "Arbitrarily shaped microstrip structures and their analysis with a mixed potential integral equation," *IEEE Trans. Microwave Theory Tech.*, vol. 36, pp. 314–323, Feb. 1988.

[9] ———, "Integral equation technique," in *Numerical Techniques for Microwave and Millimeter-Wave Passive Structures*, T. Itoh, Ed. New York: Wiley, 1989, pp. 133–214.

[10] R. W. Jackson, "Full-wave finite-element analysis of irregular microstrip discontinuities," *IEEE Trans. Microwave Theory Tech.*, vol. 37, pp. 81–89, Jan. 1989.

[11] W. P. Harokopus and P. B. Katehi, "Characterization of microstrip discontinuities on multilayer dielectric substrates including radiation losses," *IEEE Trans. Microwave Theory Tech.*, vol. 37, pp. 2058–2066, Dec. 1989.

[12] S. C. Wu, H. Y. Yang, N. G. Alexoplous, and I. Wolff, "A rigorous dispersive characterization of microstrip cross and T junction," *IEEE Trans. Microwave Theory Tech.*, vol. 38, pp. 1837–1844, Dec. 1990.

[13] T. S. Horng, N. G. Alexopoulos, S. C. Wu, and H. Y. Yang, "Full-wave spectral-domain analysis for open microstrip discontinuities of arbitrary shape including radiation and surface-wave losses," *Int. J. Microwave Millimeter-Wave Comput.-Aided Eng.*, vol. 2, no. 4, pp. 224–240, 1992.

[14] M. Kahrizi, T. K. Sarkar, and Z. A. Maricevic, "Analysis of a wide radiation slot in the ground plane of a microstrip line," *IEEE Trans. Microwave Theory Tech.*, vol. 41, pp. 29–37, Jan. 1993.

[15] X. Zhang and K. K. Mei, "Time-domain finite difference approach to the calculation of the frequency-dependent characteristics of microstrip discontinuities," *IEEE Trans. Microwave Theory Tech.*, vol. 36, pp. 1775–1787, Dec. 1988.

[16] D. M. Sheen, S. M. Ali, M. D. Abouzahra, and J. A. Kong, "Application of the three-dimensional finite-difference time-domain method to the analysis of planar microstrip circuits," *IEEE Trans. Microwave Theory Tech.*, vol. 38, pp. 849–857, July 1990.

[17] P. Gillard, J. H. Corre, M. Drissi, and J. Citerne, "A general treatment of matched terminations using integral equations-modeling and applications," *IEEE Trans. Microwave Theory Tech.*, vol. 42, pp. 2545–2552, Dec. 1994.

[18] E. K. L. Yeung, J. C. Beal, and Y. M. M. Antar, "Multilayer microstrip structure analysis with matched load simulation," *IEEE Trans. Microwave Theory Tech.*, vol. 43, pp. 143–149, Jan. 1995.

[19] G. V. Eleftheriades and R. Mosig, "On the network characterization of planar passive circuits using the method of moments," *IEEE Trans. Microwave Theory Tech.*, vol. 44, pp. 438–445, Mar. 1996.

[20] L. Zhu, E. Yamashita, and I. Joishi, "Generalized modeling of microstrip-fed patch antennas using an equivalent delta voltage source backed by a perfect electric wall," presented at the *1996 IEEE AP-S Int. Symp. and URSI Radio Sci. Meeting*, Baltimore, MD, July 21–26, 1996.

[21] S. Hashemi-Yeganeh, "On the summation of double infinite series field computations inside rectangular cavities," *IEEE Trans. Microwave Theory Tech.*, vol. 43, pp. 641–646, Mar. 1995.

[22] T. Itoh, "Spectral domain admittance approach for dispersion characteristics of generalized printed transmission lines," *IEEE Trans. Microwave Theory Tech.*, vol. MTT-28, pp. 733–736, July 1980.

Lei Zhu (S'91–M'93) received the B.Sc. and M.Sc. degrees of engineering from the Nanjing Institute of Technology (now Southeast University), Nanjing, Jiangsu, China, in 1985 and 1988, respectively, and the Ph.D. degree of engineering from the University of Electro-Communications, Tokyo, Japan, in 1993.

From 1986 to 1989, he was a Research/Teaching Assistant at Nanjing Institute of Technology, where he studied millimeter-wave components and leaky-wave antennas. From 1989 to 1993, he conducted studies on the modeling of planar transmission lines and the optimized design of their passive components. From 1993 to 1996, he was a Research Engineer with Matsushita-Kotobuki Electronics Industries, Ltd., Japan, where he conducted research/development of planar antennas for wireless communications. Since 1996, he has been a Post-Doctoral Research Associate at École Polytechnique de Montreal, Montréal, P.Q., Canada, where his main research interest is to develop EM software for the optimized design of compact planar dual-mode filters.

Dr. Zhu was awarded the Japanese Government (Monbusho) Graduate Fellowship from1989 to 1993, the First-Order Achievement Award in Science and Technology from the National Education Committee of China in 1993, and the Silver Award of Excellent Invention from the Matsushita-Kotobuki Electronics Industries, Ltd., Japan, in 1996.

Ke Wu (M'87–SM'92), photograph and biography not available at the time of publication.